Earth Science Informatics (2021) 14:2411–2421
https://doi.org/10.1007/s12145-021-00660-z

SOFTWARE ARTICLE

FKgrain: A topography-based software tool for grain segmentation and sizing using factorial kriging

Fu-Chun Wu[1] · Chi-Kuei Wang[2] · Hong Ping Lo[2]

Received: 27 February 2021 / Accepted: 22 June 2021 / Published online: 9 July 2021

Abstract
The grain size distribution (GSD) of a river bed is fundamental information required for studies of fluvial, morphological, and ecological processes. To achieve higher efficiency, numerous efforts have been devoted to developing the techniques of automated grain sizing. These techniques can be categorized as the image-based or topography-based approach according to the input data used. Each category is further subdivided into three groups based on the output result, namely: individual GSD, statistical GSD, or characteristic grain sizes. Existing software for automated grain sizing covers the image-based approaches for all three types of output, and topography-based approaches for statistical GSD and characteristic grain sizes. To date, however, no software has been developed that uses 3D topographic data to delineate individual grains and estimate their GSD. Here, we present a first-ever topography-based software tool, FKgrain, for automated grain segmentation and sizing. FKgrain adopts factorial kriging to decompose the grain-scale component of digital elevation model (DEM), whose zero-level contours are then used as the input for morphological grain segmentation. FKgrain exports the shapefiles of the delineated grains and their ellipse fits, whose minor axes can be used to derive the individual GSD. An application example demonstrates that FKgrain is efficient in producing useful results that are comparable to those obtained by traditional, time-consuming and laborious manual digitization of grain images.

Keywords Factorial kriging (FK) · Grain size distribution (GSD) · Digital elevation model (DEM) · Morphological grain segmentation

Introduction

The grain size distribution (GSD) of the river bed is fundamental information required for studies of fluvial hydraulics, sediment transport, and morphological and ecological processes (e.g., Detert and Weitbrecht, 2012; Woodget and Austrums, 2017; Purinton and Bookhagen, 2019; Lang et al., 2021). Traditional methods for acquiring the GSD, such as the mechanical sieving used in the laboratory and grid-by-number or line sampling used in the field (Wolman, 1954; Fehr, 1987), are time-consuming, laborious, costly, destructive, and limited by the spatial extent and accessibility of the sampling sites. To overcome these difficulties, researchers proposed photosieving methods that manually measure grain sizes from photographs (e.g., Ibbeken and Schleyer, 1986). Subsequently, to achieve higher efficiency, numerous efforts have been directed to the development of techniques for automated grain sizing. These techniques can be categorized as the image-based or topography-based approach according to the input data used (Table 1). Each category is further subdivided into three groups based on the output results: (1) GSD derived from all delineated grains, termed 'individual GSD'; (2) GSD derived from global statistics of image properties or bed elevation, termed 'statistical GSD'; (3) characteristic grain sizes of the sampled population (e.g., D_{50}, D_{84}, or D_{mean}).

A collection of existing software and methods developed for automated grain sizing (Table 1) shows different approaches adopted in earlier works. The image-based algorithms for the individual GSD mainly rely on the

Communicated by: H.Babaie

✉ Fu-Chun Wu
fcwu@ntu.edu.tw

1 Department of Bioenvironmental Systems Engineering and Hydrotech Research Institute, National Taiwan University, Taipei, Taiwan

2 Department of Geomatics, National Cheng Kung University, Tainan, Taiwan

Table 1 A collection of existing software and methods for automated grain sizing

Input data	Output result	Software (with download site) or method	Source
2D image	Individual GSD	***Digital Gravelometer* – Morphological image processing and watershed segmentation** (http://www.sedimetrics.com)	Graham et al. (2005a, 2005b)
		***BASEGRAIN* – Automatically detected grains converted to a quasi-sieve GSD by line sampling** (https://basement.ethz.ch/download/tools/basegrain.html)	Detert and Weitbrecht (2012, 2013)
		***PebbleCounts* – *k*-means clustering in additional image color spaces and spectral domain** (https://github.com/UP-RS-ESP/PebbleCounts)	Purinton and Bookhagen (2019)
		Morphological image processing	McEwan et al. (2000)
		Edge seeding with image porosity and partial watershed segmentation	Sime and Ferguson (2003)
	Statistical GSD	***pyDGS* – Approximating GSD by wavelet-based global power spectral density function** (https://github.com/dbuscombe-usgs/pyDGS)	Buscombe (2013)
		***SediNet* – CNN for equivalent sieve GSD w/o the need of area-to-mass conversion & image scaling** (https://github.com/MARDAScience/SediNet)	Buscombe (2020)
		***GRAINet* – UAV-based CNN for spatial GSD** (https://github.com/langnico/GRAINet)	Lang et al. (2021)
		Autocorrelation analysis of image intensity	Rubin (2004)
		Kernel density & 2D autocorrelogram field derived from image power spectrum	Buscombe (2008)
	Characteristic grain size	***Cobble Cam* – Autocorrelation analysis for D_{mean}** (https://cmgds.marine.usgs.gov/data/seds/grainsize/code.html)	Warrick et al. (2009)
		***MAGIC* – 2D spectral decomposition for D_{mean}** (https://cmgds.marine.usgs.gov/data/seds/grainsize/code.html)	Buscombe et al. (2010) Buscombe and Rubin (2012)
		Local texture & semivariance of high-resolution airborne imagery for river-scale mapping of D_{50}	Carbonneau et al. (2004)
3D topography	Individual GSD	***FKgrain* – Grain segmentation/sizing by factorial kriged DEM & morphological image processing** (https://github.com/ncku-arsem/FKgrain)	**This study**
		Combined image analysis & Hurst edge detection	Butler et al. (2001)
	Statistical GSD	***PySESA* – Spectral analysis package for spatially distributed data in spatial & frequency domains** (https://github.com/dbuscombe-usgs/pysesa/)	Buscombe (2016)
		Combined terrestrial photosieving and airborne LiDAR-derived roughness for GSD estimation	Chardon et al. (2020)
	Characteristic grain size (D_{50}, D_{84}) D_{mean}	***Point-Cloud-Tools* – Processing of TLS point clouds for patch-scale roughness vs. D_{50}** (https://code.google.com/archive/p/point-cloud-tools/)	Rychkov et al. (2012)
		***ToPCAT* – Decimation of TLS point clouds into detrended DEMs that retain subgrid topography for mapping reach-scale roughness vs. D_{50}** (http://gcd6help.joewheaton.org/gcd-concepts/topcat-decimation)	Brasington et al. (2012)
		Empirical relations for TLS-derived roughness vs. D_{mean} extracted from *a*-, *b*-, and *c*-axes	Heritage and Milan (2009)
		SfM-derived roughness vs. D_{50} relation affected by grain shape, packing, sorting, and bedform	Pearson et al. (2017)
		D_{50}, D_{84}, D_{mean} more strongly related to 3D UAV-SfM-derived roughness than to 2D image entropy	Woodget and Austrums (2017)

morphological image processing/analysis for segmentation and sizing of the resolvable grains (e.g., McEwan et al., 2000; Sime and Ferguson, 2003; Graham et al., 2005a, b; Strom et al., 2010), with additional sophistication (e.g., line sampling or *k*-means clustering) included by some researchers (Detert and Weitbrecht, 2012, 2013; Purinton and Bookhagen, 2019). In contrast, the image-based algorithms for the statistical GSD or characteristic grain sizes rely on the empirical relations between the grain sizes and statistical metrics of image intensity or texture. The statistical metrics used in these algorithms include: semivariance (Carbonneau et al., 2004), autocorrelation (Rubin, 2004; Buscombe, 2008; Warrick et al., 2009; Buscombe et al., 2010; Buscombe and Rubin, 2012), wavelet power spectrum (Buscombe, 2013), entropy (Woodget and Austrums, 2017), and convolutional-layer activation (Buscombe, 2020; Lang et al., 2021).

On the other hand, the topography-based algorithms use the 3D topographic data or digital elevation model (DEM) derived from the terrestrial or airborne LiDAR, or structure-from-motion photogrammetry. To estimate the statistical GSD or characteristic grain sizes, researchers have built correlations between the local roughness (local standard deviation) or power spectrum of DEM and the sampled grain sizes (e.g., Heritage and Milan, 2009; Rychkov et al., 2012; Brasington et al., 2012; Buscombe, 2016; Woodget and Austrums, 2017; Pearson et al., 2017; Chardon et al., 2020). Woodget and Austrums (2017) further found that the characteristic grain sizes are more closely related to the 3D topographic roughness than 2D image entropy. To date, however, no software has been developed that uses the 3D topographic data to delineate individual grains and estimate their GSD. An earlier attempt (Butler et al., 2001) was made to detect the edges of the grains by using the Hurst texture (topographic gradient) operator, it was used only to supplement a morphological image processing for grain segmentation, rather than develop a standalone topography-based algorithm for estimation of individual GSD.

To fill this methodological gap and make the software list (Table 1) more comprehensive, here we apply the factorial kriging (FK) to devise a DEM-based software tool, FKgrain, for segmentation and sizing of individual grains. FKgrain is the first of its kind that uses topographic data to estimate individual GSD and export the shapefile of grain boundaries, the latter being a long-sought product useful for delineation of microforms such as pebble clusters (Entwistle et al., 2007; Wu et al., 2018). Below, the procedure of FK is briefly summarized, followed by an overview of the software and user interface, and an application example to demonstrate the workflow and output results from each part of FKgrain.

Design and Implementation

Factorial kriging

The procedure of FK is briefly summarized here, for further details on the theory of FK method the readers are referred to Wu et al. (2018). FK decomposes the DEM into a short-range (grain-scale) component and a long-range (microform-scale) component. Prior to subsequent analyses, the original DEM is normalized to a zero mean and planar detrended to remove the large-scale bed slope (Hodge et al., 2009a, b), so that only the grain- and microform-scale topographies are retained (Huang and Wang, 2012; Wu et al., 2018). The variogram of the detrended DEM is calculated and fit with a double spherical model that integrates linearly two spherical models, one with a short range and the other with a long range. The short- and long-range spherical models are used to estimate, respectively, the short- and long-range factorial kriged (FK) DEMs. Summation of these two components yields the ordinary kriged (OK) DEM. In FKgrain, the zero-level contours of the short-range FK DEM serve as the input data used to perform morphological grain segmentation.

Overview

FKgrain contains a suite of programs developed with a combination of programing languages and libraries (Fig. 1). The software package (including the source codes, executable, user's manual, sample DEM and image) is available on GitHub repository (see Availability & Requirements section). FKgrain mainly consists of four parts: Part 1, generation of zero-contour image; Part 2, processing of zero-contour image; Part 3, multi-level grain segmentation; Part 4, production of output results. The programs are encapsulated with C# Wrapper. Part 1 implements the tasks described in Section 2.1, including the planar detrending (MATLAB), variogram calculation (gstat and sp packages of R), kriging (Fortran 77 GSLIB program) and generation of the zero-level contour image (GDAL library). Part 2 transforms the zero-contour image into a binary image of delineated grain segments, using the MATLAB functions of morphological operations. Part 3 separates the delineated grain segments into multiple size levels (C#) and fix the under- or over-segmented grains using morphological operations. Part 4 performs ellipse fitting of the delineated grains, generates attribute text file of ellipse fits (C#) and produces shapefiles of grain boundaries and ellipse fits (Google Go). The attribute table contains the coordinates (x, y) of the ellipse centers, major and minor (*a*- and *b*-) axes, and orientations of the *a*-axes. The *b*-axes are then used to determine the individual GSD (Bunte and Abt, 2001).

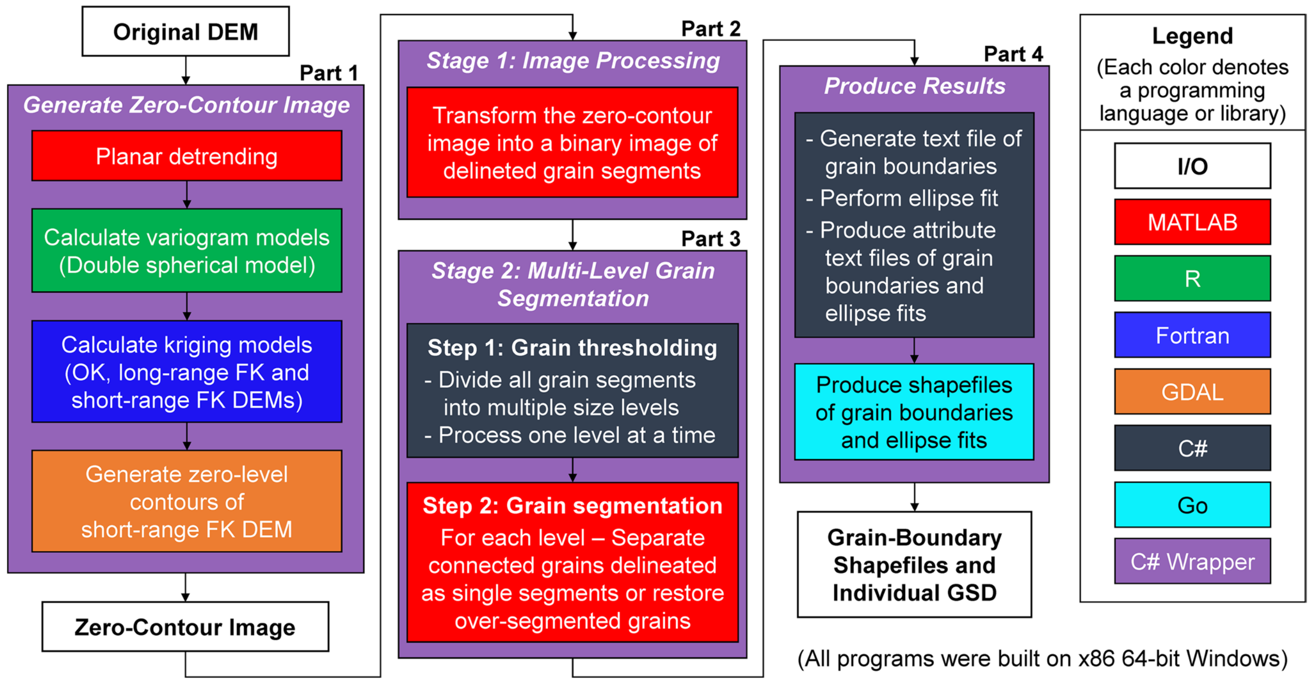

Fig. 1 Workflow of FKgrain. The software consists of four main parts that include a suite of programs developed with a combination of programing languages and libraries

User interface

After launching the executable (FKgrain.exe in software package), a menu bar with three tabs (Main, FK, and Extra) will show up (Fig. 2). Clicking FK tab and selecting "Zero-Level Contour" will lead through the tasks of Part 1. When all calculations of Part 1 are done, a set of output images (original and detrended DEMs, OK DEM, long- and short-range FK DEMs, and zero-level contours) will appear onscreen and be saved in a specified folder. These image files may be viewed by clicking FK tab and selecting "Visualization Tool" or may be retrieved by GIS software.

Given the zero-level contours, the users may proceed to Part 2 by clicking Main tab, pressing Stage 1, and selecting an input zero-contour image. A morphological operation window will show up (Fig. 2) and display a binary image of zero-level contours. On the right side of the window, the operation control panel (labeled as 1) contains several MATLAB functions of morphological operation (Inverse, Fill, Opening, Closing, Erosion, and Dilation). Through proper implementation of morphological operations, the zero-level contours are transformed into a binary image of grain segments. Operations performed during Stage 1 are displayed in the logs record panel (labeled as 2), which can be saved and retrieved for later use. The ellipse fits to the grain segments will show up automatically, which can be turned off or on (labeled as 3). For better visualization, the users may adjust the transparency or left-click on the image display to flash between the original and processed images. Press "Enter Stage 2" when all operations of Stage 1 are done.

During Stage 2, the users implement morphological grain segmentation (Part 3) by separating all grain segments into multiple size levels and processing one level at a time. Each level proceeds in two steps. Step 1 is to specify a threshold and retain only those grain segments that are greater than the threshold. The thresholded smaller segments will be processed in subsequent levels. Step 2 is to separate the connected grains that are delineated as a single segment or restore the over-segmented grains. A morphological operation window will show up, where the users can select from a list of functions to perform morphological grain segmentation. Enter the next level after a level is done. Repeat until the minimum resolvable grain size is reached at the final level.

Once all levels of grain segmentation are done, press "Save" in the dialogue box to produce and export the results (Part 4). The output results include two shapefiles: grain boundaries and ellipse fits, whose attribute tables contain the information required for derivation of the individual GSD. As an alternative, a shapefile of ellipse fits can be generated by input of a grain-boundary shapefile (e.g., manually digitized grain boundaries). This can be done by clicking Extra tab in the menu bar and selecting an input shapefile of grain boundaries.

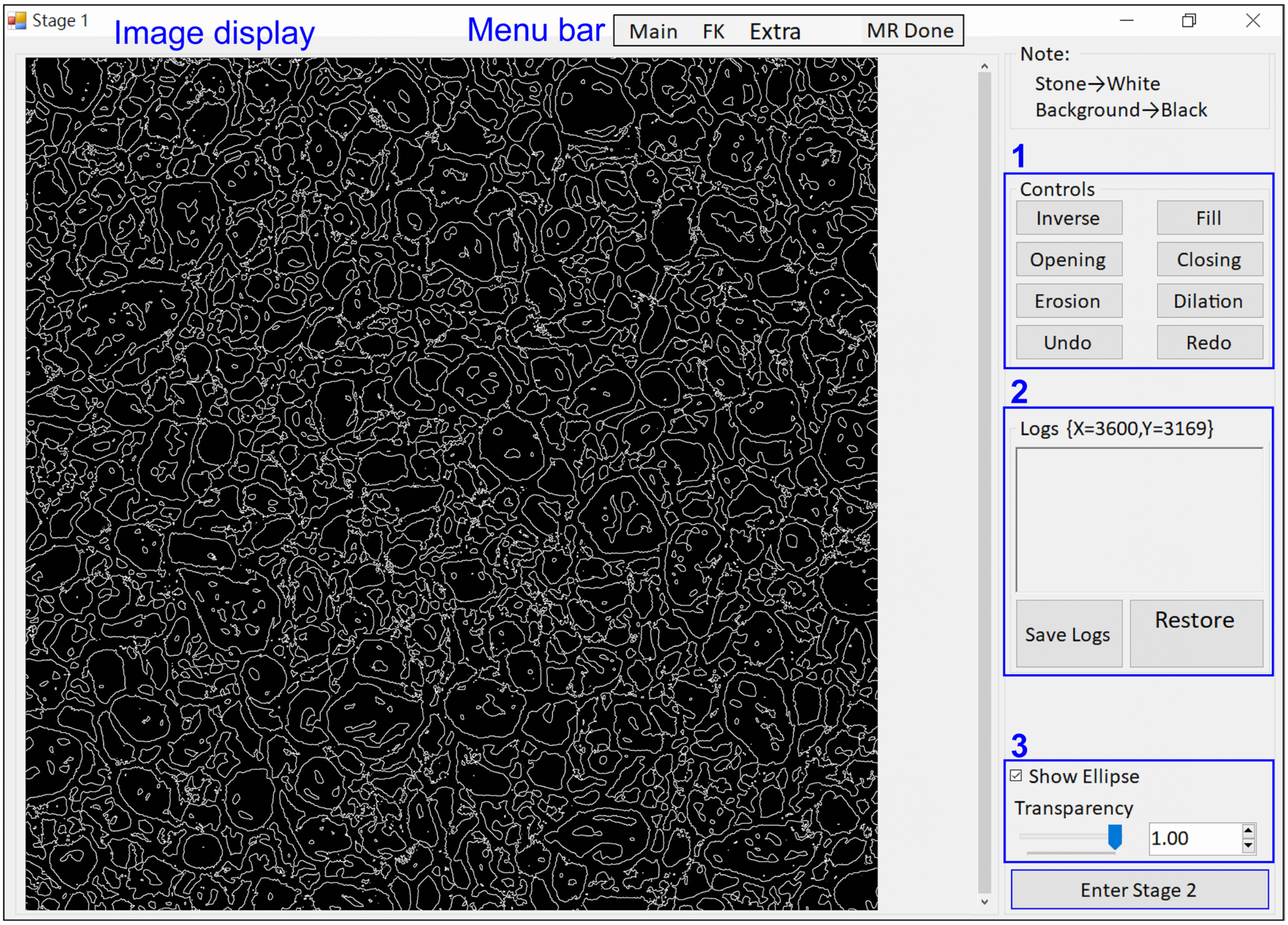

Fig. 2 Graphical user interface of FKgrain. Menu bar includes three main tabs. Morphological operation window includes a binary image display, operation control panel (labeled as 1), logs record panel (labeled as 2), and visualization control panel (labeled as 3)

Application

In this section, we demonstrate how FKgrain is applied to implementing factorial kriging and morphological grain segmentation. The DEM used here is adopted from Wu et al. (2018), which covers 6 m × 6 m patch of gravel bar scanned with terrestrial LiDAR. The resulting high-density point clouds were mapped onto 1 cm × 1 cm grids using a mean filter (Wang et al., 2011). This DEM is provided in the Sample DEM folder of the software package. The results exported by each part of FKgrain are reported in the following subsections.

Part 1 – Kriged DEM and zero-contour images

The DEM was normalized to a zero mean and planar detrended (see user's manual (Lo et al., 2021) for a full set of output images). The detrended data were processed by ordinary kriging to produce a voidless OK DEM (Fig. 3a). Factorial kriging was then implemented to generate the long- and short-range FK DEMs (Figs. 3b-c). The OK DEM is a superposition of the long- and short-range FK DEMs. The long-range FK DEM and OK DEM have similar elevation histograms (Fig. 3d), yet the former exhibits a smoother topography with no clear grain boundaries. By contrast, the short-range FK DEM exhibits a flatter topography, where > 85% of elevation data are distributed in a narrow range between ± 0.04 m (Fig. 3d). The boundaries of individual grains are distinctly outlined, where the elevation exhibits a sharp transition between positive and negative values (i.e., light and dark gray), suggesting that the zero contours of the short-range FK DEM may serve as a basis for morphological grain segmentation.

A binary image of zero-level contours is displayed in Fig. 2, which shows that the contours well outline the grains, although a few interstitial fine dots connecting individual grains require further processing. Some fragmentations arising from the texture of grain surface are also observed. Such textural features are subgrain-scale noises that are undesirable for subsequent grain segmentation. Morphological

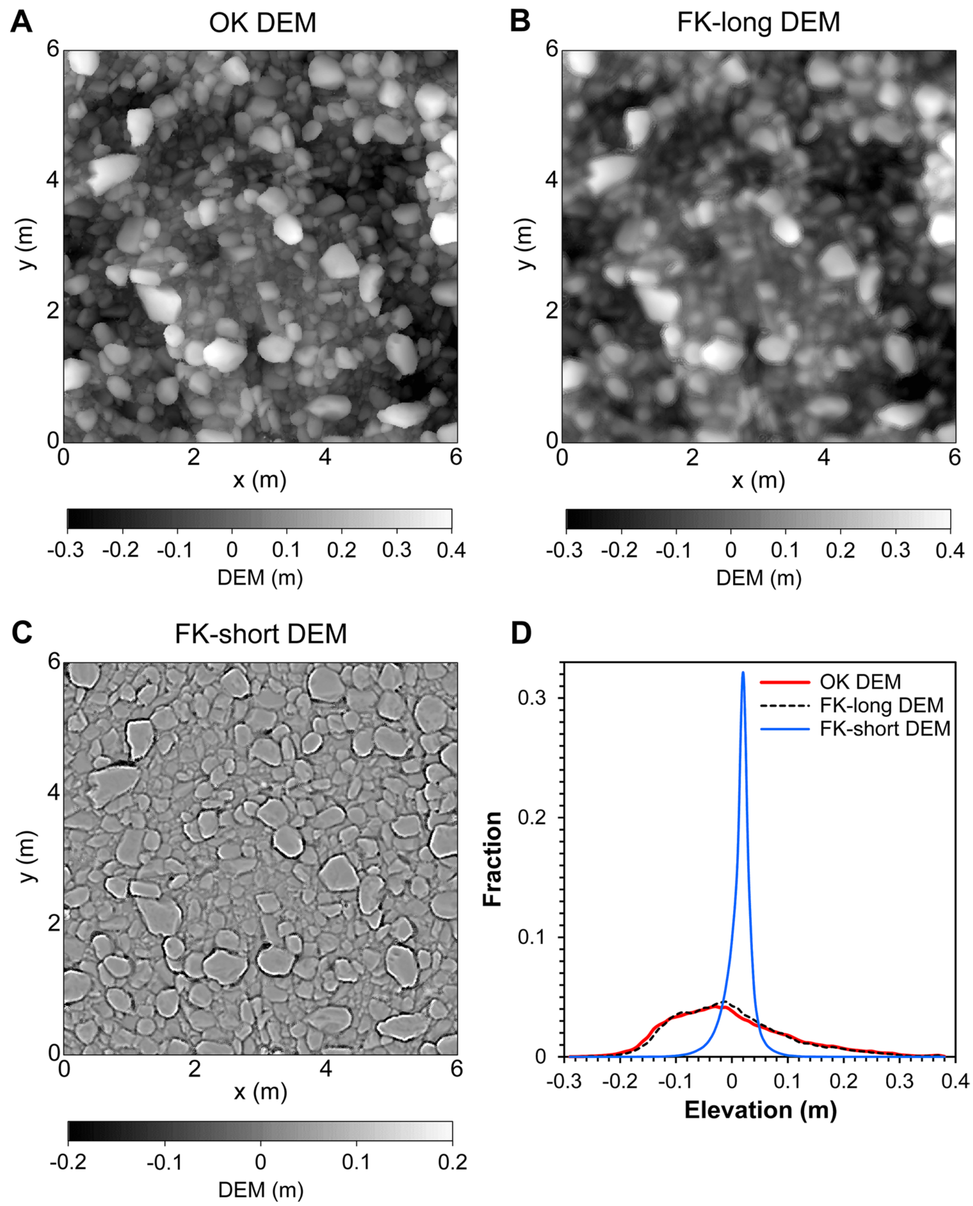

Fig. 3 Output results from Part 1 of FKgrain: (**a**) OK DEM; (**b**) long-range FK DEM; (**c**) short-range FK DEM; (**d**) elevation histograms of OK DEM, long- and short-range FK DEMs

operations are performed in the subsequent parts of FKgrain to address these issues.

Part 2 – Delineated grain segments

The zero-level contours are transformed into a binary image of grain segments by going through the following morphological operations (see user's manual (Lo et al., 2021) for detailed steps). First, use Fill function to fill the non-object background with white color, while the grain segments remain as black (Fig. 4a). Second, use Inverse function to turn the background as black and grain segments as white (Fig. 4b). Third, use Fill Holes function to remove (or fill) the fragmentations in the grains (Fig. 4c). Fourth, use Opening function (with square size = 6 pixels) to eliminate the interstitial fine dots. Note here that, by default, the original 1 cm × 1 cm resolution of DEM has been converted into four times finer (i.e., 1 pixel = 0.25 cm) when the zero-contour image was created. Fifth, use Dilation function (with square size = 4 pixels) to expand the areas of grains and reduce the excessive widths of the interstices inherited from the zero-level contours (Fig. 4d).

Care must be taken to avoid eliminating excessively the fine dots when using Opening function, or over-expanding the grain areas when using Dilation function. The parameter values given above were adjusted to optimize our segmentation results (see Part 4 below). The users may need to select parameter values that best suit their own data. For further details on Morphological Operations, the users are referred

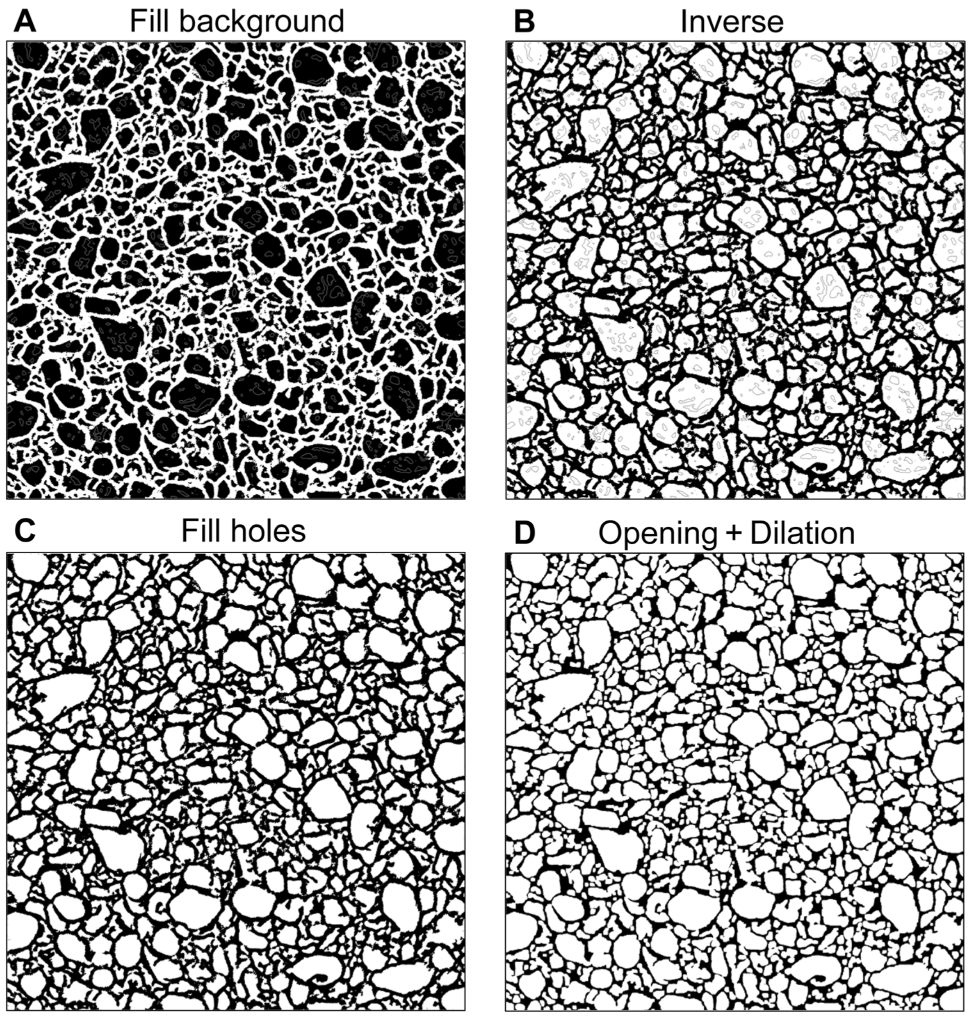

Fig. 4 Output results from Part 2 of FKgrain: (**a**) after the background was filled with white color; (**b**) after the colors of the background and grains were inverted; (**c**) after the fragmentations within the grains were filled; (**d**) after the interstitial fine dots were eliminated and the areas of grains were expanded

to the online document of MATLAB (supported by Help Center, MathWorks).

Part 3 – Multi-level grain segmentation

The result shown in Fig. 4d contains 843 grain segments, their areas range from 66 to 53,105 pixels, which, respectively, correspond to the minimum resolvable grain size (20 mm) and 580 mm. Three thresholds of segment area in descending order (5400, 540, 66 pixels) were used to divide the population, resulting in 207, 421, and 215 grain segments in Levels 1 to 3 (Figs. 5a-c), which were aimed at 1:2:1 ratio of segment numbers in the large-, medium-, and small-size classes. As shown in Figs. 5a-b, some connected grains were delineated as single segments (bounded by single ellipse fits). These were separated using Opening function, with square sizes = 19 and 13 pixels for the large- and medium-size classes (Figs. 5d-e). For the small-size class, Closing function (with square size = 7 pixels) was used to restore the over-segmented grains (Fig. 5f). After 3-level segmentation, the result contains 942 grains (Fig. 6a), where individual grains are demarcated by white lines.

Part 4 – Grain boundaries, ellipse fits, and GSD

The FKgrain-delineated boundaries outline individual grains that are identifiable in the DEM image (Fig. 6a). In a few places the shapes of the delineated grains appear incomplete, e.g., small deficiencies at the edges, yet the grain sizes extracted from the *b*-axes of the ellipse fits are deemed relatively unaffected (Fig. 6b). The sizes (*b*-axes) of the FKgrain-delineated grains range from 20 to 540 mm, coherent with the range evaluated from the manually digitized grains (i.e., 20 to 570 mm). The manually digitized result tends to include more of the smallest grains present in the interstices (Fig. 6c), which characterize the features not identified with the zero-level contours or morphological operations. The FKgrain-derived GSD is shown in Fig. 7 along with the GSD of manually digitized grains. In general, the FKgrain-derived GSD is in good agreement with the manually digitized result. As noted above, manual

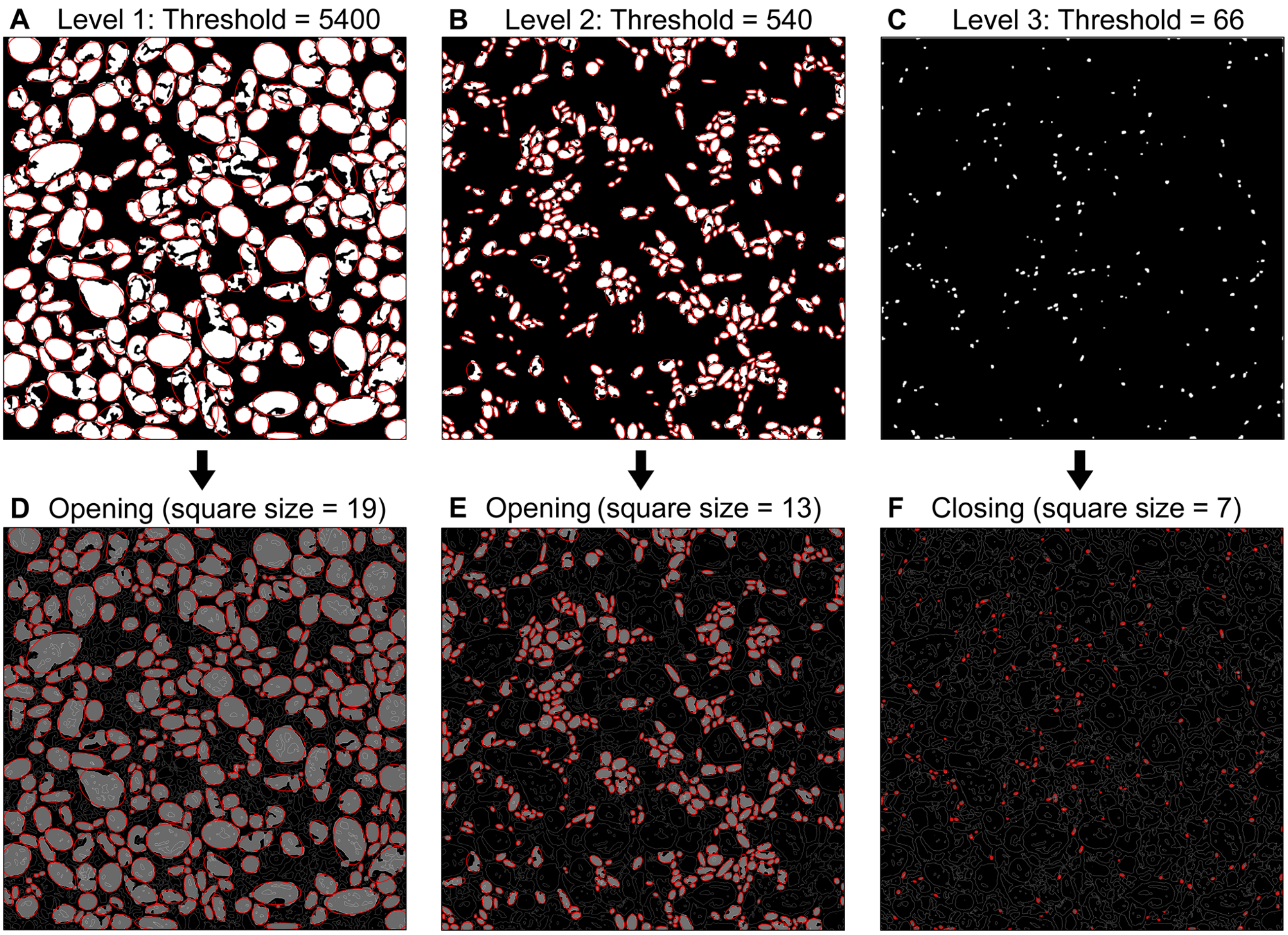

Fig. 5 Output results from Part 3 of FKgrain: (**a**) Level 1: threshold = 5400 pixels, overlaid with ellipse fits; (**b**) Level 2: threshold = 540 pixels, overlaid with ellipse fits; (**c**) Level 3: threshold = 66 pixels; (**d**) Level 1: delineated grains and ellipse fits, Opening with square = 19 pixels; (**e**) Level 2: delineated grains and ellipse fits, Opening with square = 13 pixels; (**f**) Level 3: delineated grains and ellipse fits, Closing with square = 7 pixels

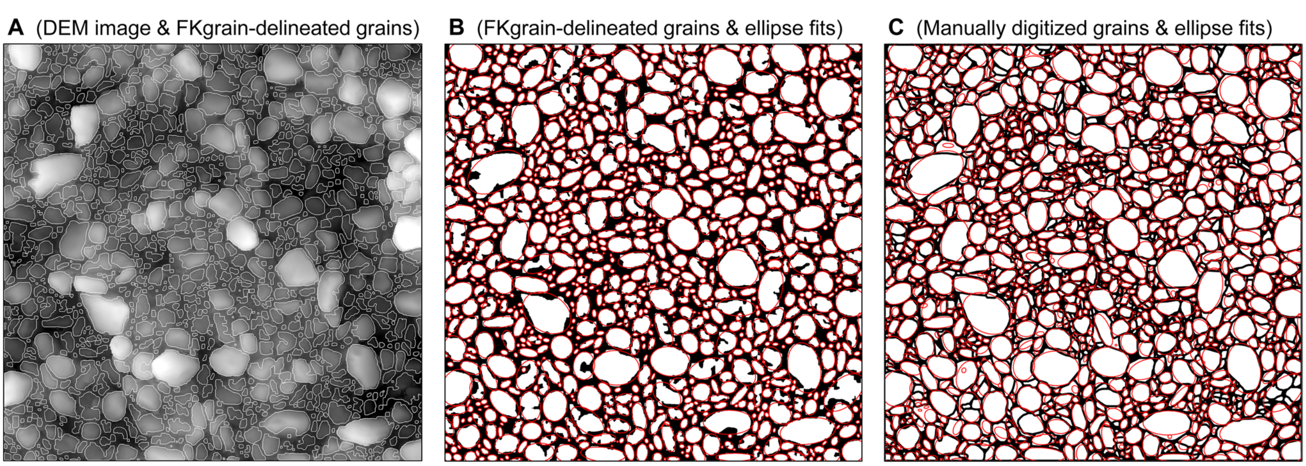

Fig. 6 Output results from Part 4 of FKgrain: (**a**) DEM image overlaid with FKgrain-delineated grain boundaries; (**b**) FKgrain-delineated grains overlaid with ellipse fits; (**c**) manually digitized grains overlaid with ellipse fits to FKgrain-delineated grains

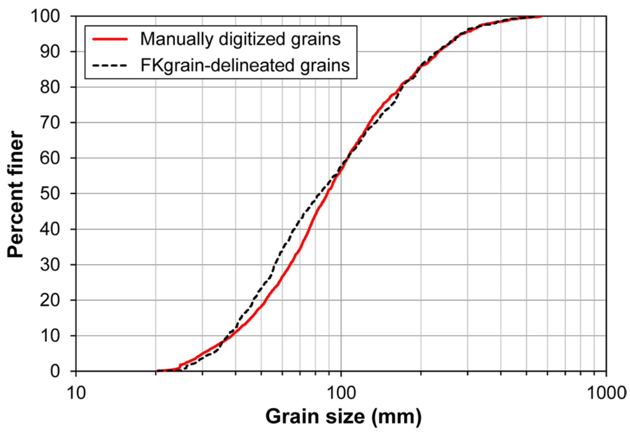

Fig. 7 Comparison between the GSDs of the FKgrain-delineated and manually digitized grains

digitization tends to account relatively more grains in the size range 20 to 40 mm, while the FKgrain-derived GSD has relatively more grains in the size range 40 to 100 mm. For grain sizes > 100 mm, however, the two GSDs exhibit close resemblance.

Quantitatively, the median grain size of the FKgrain-derived GSD ($D_{50} = 83$ mm) is concordant with D_{50} (= 89 mm) of the manually digitized grains. The sorting coefficients σ_I are 1.01 and 1.00 ($= |\phi_{84} - \phi_{16}|/4 + |\phi_{95} - \phi_5|/6.6$, where $\phi_i = \log_2 D_i$) for the FKgrain-derived and manually digitized GSDs, and the corresponding sorting indices *SI* are 2.13 and 2.01 ($= (D_{84}/D_{50} + D_{50}/D_{16})/2$). The river bed analyzed in this example is thus classified as moderately to poorly sorted (Bunte and Abt, 2001). Overall, FKgrain can efficiently implement grain segmentation and sizing and produce results that are consistent with those obtained by the time-consuming, labor-intensive manual digitization.

Discussion

Despite that many software tools exist for automated grain segmentation and sizing, FKgrain is the first of its kind using 3D topographic data to estimate individual GSD and export the shapefile of grain boundaries. This new software adopts factorial kriging to decompose the DEM into grain-scale and microform-scale components. The zero-level contours of the grain-scale component are used for morphological grain segmentation. The shapefile of grain boundaries is also useful for delineation of microforms (e.g., pebble clusters). The minor axes of the ellipse fit to the delineated grains are used to derive the individual GSD. Such knowledge is crucial for numerous applications in river science, management, and sustainable development, e.g., to obtain roughness estimates for hydraulic models, to quantify sediment erosion, transport, and deposition, to perform morphodynamic modeling/studies, to classify aquatic habitats, to assess anthropogenic impacts, and to evaluate geological deposits (e.g., Detert and Weitbrecht, 2012; Woodget and Austrums, 2017; Purinton and Bookhagen, 2019; Lang et al., 2021). Efficient, accurate estimation and mapping of riverbed GSD, supported by FKgrain, will facilitate progresses in these disciplines.

Although no upper bound has been set, the maximum area that can be processed by FKgrain is determined chiefly by the CPU (or CPU time allowed). There are two tasks in FKgrain that require intensive use of CPU: (1) calculation of variogram, and (2) generation of FK DEMs. The first task is to compute the semivariance of DEM between all paired grids for a full range of spatial lag *h* (i.e., separation distance). The second task is to generate the short- and long-range FK DEMs by solving a system of $2(N+1)$ equations at each grid point, where *N* is the number of data pairs separated by lag *h*. For instance, in the application example presented above, 6 m × 6 m area with 1 cm grid resolution requires 17 min of CPU time (10 min for task 1; 6 min for task 2), using a PC with Intel Core i7-7700 K 4.20 GHz CPU and 32 GB RAM. With the same grid resolution, 12 m × 12 m area (i.e., 4 times of 6 m × 6 m area) requires ~ 2 h of CPU time (92 min for task 1; 31 min for task 2), and 18 m × 18 m area (i.e., 9 times of 6 m × 6 m area) requires ~ 5 h of CPU time (230 min for task 1; 73 min for task 2). The required CPU time increases with the amount of data to be processed, with the linear trends of individual tasks having different slopes. The slope is greatest for the CPU time of task 1 (= 2.73), followed by the slope of the total CPU time (= 2.12), and then the slope for the CPU time of task 2 (= 1.39).

Conclusion

We present here a DEM-based software tool, FKgrain, for segmentation and sizing of riverbed sediment particles. The unique feature of FKgrain is that it adopts factorial kriging to decompose the grain-scale component of DEM, whose zero-level contours serve as the basis for morphological grain segmentation. FKgrain is the first ever software tool that uses 3D topographic data to delineate individual grains and estimate their GSD, and exports the shapefiles of delineated grain boundaries. An application example demonstrates that FKgrain is efficient in producing useful results that are concordant with those obtained by traditional time-consuming, laborious manual digitization.

We hope FKgrain will provide a tool to facilitate the full use of hyper-resolution DEM that has become increasingly accessible with the advent of laser scanning and photogrammetry technologies. FKgrain will be updated and modified persistently. We welcome feedback from the users that helps improve the functionality, implementation, and user interface of the software.

Availability and Requirements FKgrain software package, including the source codes, executable, user's manual, sample DEM and image files, are available on GitHub: https://github.com/ncku-arsem/FKgrain. FKgrain runs with Matlab Runtime, R and GDAL. The users need to download and install these dependencies following the procedure described in the user's manual. FKgrain was built on × 86 64-bit Windows, requiring at least 2 GB RAM to implement the full suite of programs.

Acknowledgements This work was supported by the Ministry of Science and Technology (MOST), Taiwan, granted to FCW (106-2221-E-002 -074 -MY3). We thank Guo-Hao Huang for the source codes of FK used in Part 1 of the software. Comments and suggestions from anonymous reviewers are acknowledged.

Authors' contributions Fu-Chun Wu contributes to research conception, supervision of software development, result analysis and interpretation, writing and editing manuscript, revisiting user's manual, and funding acquisition. Chi-Kuei Wang contributes to data acquisition, methodology, supervision of software development, drafting user's manual, and resources provision. Hong Ping Lo contributes to software coding and implementation, preparing and drafting user's manual. All authors approve the manuscript version submitted and take intellectual responsibility for its content.

Funding This research was supported by the Ministry of Science and Technology (MOST), Taiwan, granted to Fu-Chun Wu (Grant number: 106–2221-E-002 -074 -MY3).

Data availability The data/material used in this work are available on GitHub: https://github.com/ncku-arsem/FKgrain.

Code availability The source codes and executable are available on GitHub: https://github.com/ncku-arsem/FKgrain.

Declarations

Conflicts of interest/Competing interests The authors declare no conflict of interest.

References

Brasington J, Vericat D, Rychkov I (2012) Modeling river bed morphology, roughness, and surface sedimentology using high resolution terrestrial laser scanning. Water Resour Res 48:W11519. https://doi.org/10.1029/2012WR012223

Bunte K, Abt SR (2001) Sampling surface and subsurface particle-size distributions in wadable gravel- and cobble-bed streams for analysis in sediment transport, hydraulics, and streambed monitoring. General Technical Report RMRS-GTR-74. USDA Forest Service, Rocky Mountain Research Station, Fort Collins, CO, p 428. https://www.fs.usda.gov/treesearch/pubs/4580

Buscombe D (2008) Estimation of grain-size distributions and associated parameters from digital images of sediment. Sed Geol 210:1–10

Buscombe D (2013) Transferable wavelet method for grain-size distribution from images of sediment surfaces and thin sections, and other natural granular patterns. Sedimentology 60:1709–1732

Buscombe D (2016) Spatially explicit spectral analysis of point clouds and geospatial data. Comput Geosci 86:92–108

Buscombe D (2020) SediNet: a configurable deep learning model for mixed qualitative and quantitative optical granulometry. Earth Surf Process Landforms 45:638–651

Buscombe D, Rubin DM, Warrick JA (2010) A universal approximation of grain size from images of noncohesive sediment. J Geophys Res 115:F02015. https://doi.org/10.1029/2009JF001477

Buscombe D, Rubin DM (2012) Advances in the simulation and automated measurement of well-sorted granular material: 2. Direct measures of particle properties. J Geophys Res 117:F02002. https://doi.org/10.1029/2011JF001975

Butler JB, Lane SN, Chandler JH (2001) Automated extraction of grain-size data from gravel surfaces using digital image processing. J Hydraul Res 39:519–529

Carbonneau PE, Lane SN, Bergeron NE (2004) Catchment-scale mapping of surface grain size in gravel bed rivers using airborne digital imagery. Water Resour Res 40:W07202. https://doi.org/10.1029/2003WR002759

Chardon V, Schmitt L, Piégay H, Lague D (2020) Use of terrestrial photosieving and airborne topographic LiDAR to assess bed grain size in large rivers: a study on the Rhine River. Earth Surf Process Landforms 45:2314–2330

Detert M, Weitbrecht V (2012) Automatic object detection to analyze the geometry of gravel grains – a free stand- alone tool. In: Muños RM (ed) River flow 2012. Taylor & Francis, pp 595–600. https://www.taylorfrancis.com/books/mono/10.1201/b13250/river-flow-2012-rafael-murillo-munoz

Detert M, Weitbrecht V (2013) User guide to gravelometric image analysis by BASEGRAIN. In: Fukuoka S, Nakagawa H, Sumi T, Zhang H (eds) Advances in river sediment research. Taylor & Francis, pp 1789–1795. https://www.taylorfrancis.com/books/mono/10.1201/b15374/advances-riversediment-research-shoji-fukuoka-hajime-nakagawa-tetsuya-sumi-hao-zhang

Entwistle NS, Heritage GL, Johnson K, Hetherington D (2007) Repeat terrestrial laser scanner survey of pebble cluster creation and formation in response to flow change. Proceedings of the Annual Conference. Remote Sensing and Photogrammetry Society, Nottingham

Fehr R (1987) Einfache Bestimmung der Korngrössenverteilung von Geschiebematerial mit Hilfe der Linienzahlanalyse [Simple detection of grain size distribution of sediment material using line-count analysis]. Schweizer Ingenieur Und Architekt 105:1104–1109 ((**in German**))

Graham DJ, Reid I, Rice SP (2005a) Automated sizing of coarse-grained sediments: Image-processing procedures. Math Geol 37:1–28

Graham DJ, Rice SP, Reid I (2005b) A transferable method for the automated grain sizing of river gravels. Water Resour Res 41:W07020. https://doi.org/10.1029/2004WR003868

Heritage GL, Milan DJ (2009) Terrestrial Laser Scanning of grain roughness in a gravel-bed river. Geomorphology 113:4–11

Hodge R, Brasington J, Richards K (2009a) Analysing laser-scanned digital terrain models of gravel bed surfaces: linking morphology to sediment transport processes and hydraulics. Sedimentology 56:2024–2043

Hodge R, Brasington J, Richards K (2009b) In situ characterization of grain-scale fluvial morphology using Terrestrial Laser Scanning. Earth Surf Process Landforms 34:954–968

Huang G-H, Wang C-K (2012) Multiscale geostatistical estimation of gravel-bed roughness from terrestrial and airborne laser scanning. IEEE Geosci Remote Sens Lett 9:1084–1088

Ibbeken H, Schleyer R (1986) Photo-sieving: a method for grain-size analysis of coarse-grained, unconsolidated bedding surfaces. Earth Surf Proc Land 11:59–77

Lang N, Irniger A, Rozniak A, Hunziker R, Wegner JD, Schindler K (2021) GRAINet: Mapping grain size distributions in river beds from UAV images with convolutional neural networks. Hydrol Earth Syst Sci 25:2567–2597

Lo HP, Wang C-K, Wu F-C (2021) FKgrain user's manual (version 2021/6/8). https://github.com/ncku-arsem/FKgrain. Accessed 10 June 2021

McEwan IK, Sheen TM, Cunningham GJ, Allen AR (2000) Estimating the size composition of sediment surfaces through image analysis. Proc. Instn Civ. Engrs Water & Mar Engng 142:189–195

Pearson E, Smith MW, Klaar MJ, Brown LE (2017) Can high resolution 3D topographic surveys provide reliable grain size estimates in gravel bed rivers? Geomorphology 293:143–155

Purinton B, Bookhagen B (2019) Introducing PebbleCounts: a grain-sizing tool for photo surveys of dynamic gravel-bed rivers. Earth Surf Dynam 7:859–877. https://doi.org/10.5194/esurf-7-859-2019

Rubin DM (2004) A simple autocorrelation algorithm for determining grain size from digital images of sediment. J Sediment Res 74:160–165

Rychkov I, Brasington J, Vericat D (2012) Computational and methodological aspects of terrestrial surface analysis based on point clouds. Comput Geosci 42:64–70

Sime LC, Ferguson RI (2003) Information on grain sizes in gravel-bed rivers by automated image analysis. J Sediment Res 73:630–636

Strom KB, Kuhns RD, Lucas HJ (2010) Comparison of automated image-based grain sizing to standard pebble-count methods. J Hydraul Eng 136:461–473

Wang C-K, Wu F-C, Huang G-H, Lee C-Y (2011) Mesoscale terrestrial laser scanning of fluvial gravel surfaces. IEEE Geosci Remote Sens Lett 8:1075–1079

Warrick JA, Rubin DM, Ruggiero P, Harney JN, Draut AE, Buscombe D (2009) Cobble cam: grain-size measurements of sand to boulder from digital photographs and autocorrelation analyses. Earth Surf Process Landforms 34:1811–1821

Wolman MG (1954) A method of sampling coarse river-bed material. EOS Trans Am Geophys Union 35:951–956

Woodget AS, Austrums R (2017) Subaerial gravel size measurement using topographic data derived from a UAV-SfM approach. Earth Surf Process Landforms 42:1434–1443

Wu F-C, Wang C-K, Huang G-H (2018) Delineation of gravel-bed clusters via factorial kriging. Geomorphology 308:161–174